Article

Not peer-reviewed version

Optimization and Efficiency Enhancement of Modified Polymer Solar cells

Muhammad Raheel Khan * and Bożena Jarząbek *

Posted Date: 11 August 2023

doi: 10.20944/preprints202308.0912.v1

Keywords: Polymer thin films; BHJ organic solar cells; Hole transport layer (HTL); Electron transport layer (ETL); Reflection coating; SCAPS-1D simulation

Article

Optimization and Efficiency Enhancement of Modified Polymer Solar Cells

Muhammad Raheel Khan * and Bożena Jarząbek *

Centre of Polymer and Carbon Materials, Polish Academy of Sciences, ul. Sklodowskiej-Curie 34, 41-819 Zabrze, Poland; bjarzabek@cmpw-pan.pl

* Correspondence: khattakraheel41@gmai.com (M.R.K.); bjarzabek@cmpw-pan.pl (B.J.)

Abstract: In this study organic bulk heterojunction (BHJ) solar cell along with the spiro OMeTAD as a hole transport layer (HTL) and the PDINO as an electron transport layer (ETL) was simulated through the Solar Capacitance Simulator, one dimensional (SCAPS-1D) software to examine the performance of this type of polymer thin film organic solar cells. As an active layer the blend of polymer donor PBDB-T and non-fullerene acceptor ITIC-OE was used. Numerical simulation was performed by varying the thickness of HTL and active layer. Firstly, the HTL layer thickness was optimized to 50 nm, after that the active layer thickness varied up to 80 nm. These results of simulation demonstrated that the HTL thickness has rather little impact on efficiency while in the case of active layer thickness improves efficiency significantly. The temperature effect on the performance of solar cells was considered, by the simulation performed for temperature from 300 K up to 400 K and the efficiency of solar cell decreases with increasing temperature. Generally, polymer films usually are full of traps and defects, the density of defects (Nt) value was also introduced to the simulation, and it was confirmed that with the increasing of defect density (Nt), the efficiency of solar cell decreases. After thickness, temperature and defect density optimization, the reflection coating was also applied on it. It turned out that by introducing the reflection coating on the back side of solar cell, the efficiency increases by 2.5 %. Additionally, the positive effect of HTL and ETL doping on efficiency of this type of solar cells was demonstrated.

Keywords: polymer thin films; BHJ organic solar cells; Hole transport layer (HTL); electron transport layer (ETL); reflection coating; SCAPS-1D simulation

1. Introduction

Organic semiconductors and polymers have gained attention for many years, as an interesting material, suitable for optoelectronic, especially for organic solar cells. Among the renewable energy technologies, 3rd generation solar cell is the finest technology and has potential to replace silicon based solar cell [1–5]. Organic semiconductors have the advantage comparable to silicon solar cells i.e., light weight, flexible, low cost, and tunable processing at room temperature [6,7]. Silicon solar cells efficiency and stability are still greater than for organic solar cells (OSC) but in future it may be increased by using a suitable absorber layer. To improve the power conversion efficiency (PCE) of polymer organic thin film solar cell, different techniques have been used by the researcher [8–10].

In an OSC, the HTL and ETL are essential components along with the active layer. The HTL facilitates the movement of positive charge carriers (holes) generated by the absorption of light in the active layer, towards the anode. These layers usually consist of materials that efficiently transport holes and good compatibility with adjacent layers. The ETL on the other hand, enables the movement of negative charge carriers (electrons) generated in the active layer, towards the cathode. Like the HTL ,the ETL is designed with materials that have excellent electron mobility and interface compatibility. The active layer consists of photoactive materials. When light is incident on this layer, it absorbs photons and generates electron-hole pairs. The efficient separation and transportation of these charge carriers to their respective electrodes (anode and cathode) by the HTL and ETL lead to the conversion of light energy into electrical energy in the OSC. Some scientists have reached the conclusion that by using an appropriate combination of ETL, HTL, and a blend of donor and acceptor materials, as an active layer, may give an excellent photovoltaic response [11–13]. The scientific

 doi:10.20944/preprints202308.0912.v1

community has shown significant interest in BHJ solar cells due to their numerous advantages, such as being lightweight, cost-effective, having a tunable band gap, and displaying relatively good power conversion efficiency (PCE) [14]. The non-fullerene acceptor (NFA) has also gained considerable attention from researchers, thanks to its achieved high efficiency, reaching around 18% [15–17]. Compared to the fullerene acceptor (FA), the NFA surpasses all the drawbacks observed in FA when integrated into a BHJ structure. NFA offers an easily synthesized process, exhibits good visible and near-infrared (NIR) absorption, and according to Ma et al. [18], it boosts long-term stability, unlike FA.

A group of researchers [19] has developed an OSC incorporating with NFA by employing PBDB-T as a donor while the ITIC-OE is used as an acceptor. The efficiency of this solar cell is reported as 8.5 % [19]. By adding oligoethylene (OE) side chains to the blend can improve NFA dielectric constant up to 6.1. Generally, organic semiconductors have high exciton binding energy, due to the low dielectric constant values which increases the recombination at interface [20].

Different photovoltaic organic BHJ structures have been investigated and presented in numerous publications. Shabaz et.al presented a work [21] on new energetic indandione containing planer donor to enhance stability and efficiency of OSC. In this article they presented a novel and energetic indandione containing donor molecule to boost the performance of BHJ. H3T-1D donor molecule has an optical band gap (Eg) of approximately 1.98 eV, while [6,6]-phenyl C61 butyric acid methyl ester (PC61BM) is utilized as acceptor. The photovoltaic characteristics of BHJ based solar cells measured and discussed in [21], where the fabricated solar cell has PCE 4.05 %, short current density (J_{sc}) 10.43 $mAcm^{-2}$, open circuit voltage (V_{oc}) of 0.77V, and 0.51 fill factor (FF). Another paper [22] on a symmetric benzo-selena-diazole based donor-acceptor-donor (D-A-D) molecule for BHJ solution processed OSC is presented by the researcher. In this work they synthesized a novel organic compound with D-A-D structure such as (RTh-BSe-ThR). Benzoselenadiazole is used as an acceptor while hexylbithiophene is employed as a donor unit by multistep synthetic pathways. The synthesized RTh-BSe-ThR chromophore exhibits improved absorption with a relatively lower Eg of approximately 1.87 eV and has optimum HOMO / LOMO energy levels. The experimental result shows that the addition of Se atoms to the chromophore, improves the relevant photovoltaic performance parameters of BHJ-OSC. RTh-BSe-ThR chromophore is blended with PC61BM with different ratios such as 1:1 w / w, 1:2 w / w, 1:3 w / w and 1:4 w / w and has calculated the photovoltaic parameters for different ratios. The optimized and highest efficiency is obtained by using 1:3 w / w with Jsc 11.2 (mA / cm^2), Voc 6.684, FF 45 (%) and PCE 3.61 %. The highest efficiency is due to the light harvesting ability of active layer, exciton dissociation and charge transport active layer interface.

As compared to experimental works, simulation studies are also important. Through the simulation study we investigate how the device parameters can affect the physical properties and how the solar cells performance can be improved. Numerous literatures are now available related to simulation study for the 3rd generation solar cells; however rare research studies have been conducted on OSCs simulation. Abdelaziz et.al [23], presented a research paper on potential efficiency enhancement of NFA based solar cell through device simulation. NFA attract the scientific community owing to the relatively higher stability and efficiency. SCAPS simulation was used in [23], to perform the J-V characteristic and compared these values to the available literature. The simulation of solar cells shows higher efficiency i.e., 14.25% which is close to the reported literature values. The matching characteristic confirms that SCAPS software can be used as a standardized tool for simulation studies of OSC including NFA. In [1] authors developed and optimized a novel design of poly [[4,8-bis [(2-ethylhexyl)oxy]benzo[1,2-b:4,5-b']dithiophene-2,6-diyl][3-fluoro-2-[(2-ethylhexyl)carbonyl]thieno[3,4-b]thiophenediyl]] [6,6]-phenyl-C71-butyric acid methyl ester (PTB7: PC70BM) by using PEDOT: PSS as a HTL while the Poly[(9,9-bis(3'-((N,N-dimethyl)-N-ethylammonium)-propyl)-2,7-fluorene)-alt-2,7-(9,9-dioctylfluorene)] dibromide (PFN: Br) is used as an ETL. They concluded that optimized solar cell has a J_{sc} 16.434 $mA.cm^{-2}$, FF 68.055 %, V_{oc} 0.731 and the efficiency is reported as 8% [1]. Polymers are full of traps, so in this simulation they introduced defect density at the cell layers to yield more realistic simulations. Graphene oxide (GO), has gained attention due to its remarkable electrical, optical, and mechanical characteristics in solar cell research.

Preprints (www.preprints.org) | NOT PEER-REVIEWED | Posted: 11 August 2023 doi:10.20944/preprints202308.0912.v1

In [24] researchers used two absorber layers in their study, such as PBDB-T/ITIC and PTB7:PC70BM and have absorbed material, which interact more strongly with GO. Numerical simulation is performed by using SCAPS software by varying the thickness of absorption layer,defect density, and doping values and doping values and the solar cell is optimized to achieve the best possible efficiency of PBDB-T/ITIC solar cell by using GO, is reached as 17.34% [24] . These simulation results provide a path for GO based solar cell development. In [25] authors performed a simulation study on inverted organic solar cells. It is observed that PCE increases from 4.88 % to 5.7 % by applying P3HT and PTB7 while further increased by replacing PEDOT: PSS with MoO_3 , up to 5.92 % in best case. They suggested that increasing the efficiency above 10%, can be obtained by nanocomposites or nanoparticles addition to the polymer active layer. Mostly, the Poly(3,4-ethylenedioxythiophene) polystyrene sulfonate (PEDOT:PSS) is used commonly as an HTL in conventional solar cells because of its better conductivity and improved transparency. However, PEDOT:PSS is acidic in nature and degrades the device. Nithya et.al [26] replaced the PEDOT:PSS with Copper iodide (CuI) and carried out a simulation study for PBDB-T: ITIC by employing SCAPS – 1D software. Efficiency for this optimized structure is reported as 15.68 % and these values are encouraging, and probably the CUI can be used soon in real structures such as HTL.

The aim of this paper is to investigate the performance of thin film (PBDB-T: ITIC-OE) based OSCs. ITIC-OE shows similar optical properties to ITIC while the dielectric constant of this version with oligoethylene (OE) is higher than for ITIC. Higher dielectric constant reduces the recombination rate of charge carrier and increases the overall performance in organic solar cells, which results in the increase of photovoltaic properties namely V_{oc}, J_{sc} and PCE. In previous studies the (PEDOT:PSS) layer in photovoltaic structure was widely used. While in our studies, we replaced PEDOT: PSS with the spiro OMeTAD type HTL. PEDOT:PSS is acidic in nature and has stability problems in the PV structure. In this work the solar cell active layer thickness, defect density, HTL and ETL doping level are optimized to achieve better efficiency. Temperature has a noticeable effect on the performance of solar cells, so simulations are carried out for different temperatures from 300 K to 400 K . To the best of our knowledge so far, no studies have been found regarding the efficiency improvement through the reflection coating for high dielectric constant organic solar cells. In this work backside reflection coating is introduced, which increases efficiency by 2.5 %.

2. Materials and Methods

2.1. SCAPS 1D-Software and Mathematical Modeling

Several types of simulation software can simulate the design of photovoltaic systems i.e., SAM, RET-Screen and PV-syst. For third generation solar cells, the most popular and useful is SCAPS-1D software.This special software is invented by Ghent University Belgium to simulate the J-V characteristics and quantum efficiencies. SCAPS 1D is free and reliable open access software. Many authors have presented their simulation as well as experimental results for the polymer or organic materials by using polymer as an absorber or ETL/HTL layer. Therefore, we chose the SCAPS 1D software for the simulation of polymer thin film BHJ solar cell. To evaluate the output performance of of the solar cells, the following mathematical equations are used [27,28].

Poisson Equation:

$$\frac{\partial^2 \varphi}{\partial^2 x} = -\frac{\partial E}{\partial x} = \frac{\rho}{\varepsilon_s} = \frac{q}{\varepsilon_s}\left[\, p - n + N_D(x) - N_A(x) \pm N_{del}(x)\right] \qquad (1)$$

Transport Equation

$$J_{n,p} = nq\mu_n E + qD_n \frac{\partial n}{\partial x} + pq\mu_p E + qD_p \frac{\partial p}{\partial x} \qquad (2)$$

Continuity Equation

$$\frac{\partial n,p}{\partial t} = \frac{1}{q}\frac{J_n}{\partial x} + (G_n - R_n) + \frac{1}{q}\frac{J_p}{\partial x} + (G_p - R_p) \qquad (3)$$

Preprints (www.preprints.org) | NOT PEER-REVIEWED | Posted: 11 August 2023 doi:10.20944/preprints202308.0912.v1

Diffusion Length

$$L_{n,p} = \sqrt{D_{p,n}\,\tau_{n,p}} \quad (4)$$

Diffusivity

$$D_{p,n} = \left[\left(\frac{K_B T}{q}\right)\mu_{n,p}\right] \quad (5)$$

Open Circuit Voltage

$$V_{OC} = \frac{nK_B T}{q}\left[I_n\left(\frac{I_L}{I_0}+1\right)\right] \quad (6)$$

In the equations φ, ε represent electrostatic potential and permittivity, respectively while ρ and q represent density and elementary charge, E is an electric field. N_D and N_A represents densities of donor and acceptor.

Symbols D_n, D_p, $J_{n,p}$, μ_n, μ_p represent electron and hole diffusion coefficients, current densities, and motilities, G_n, G_p mean the generation rate for electron and hole, while recombination rate for electron/hole is represented by R_n, R_P respectively. The electron/hole lifetime is described by $\tau_{n,p}$ and the expression $\frac{K_B T}{q}$ represents the thermal voltage, and I_L, I_0 represent current generation by light and saturation current respectively.

In the context of this research, all these simulations are performed under standard test conditions (STCs). The standard conditions are the air mass 1.5 G, temperature 300 K and irradiance 1000 W.m^{-2}.

2.2. Device Architecture

Herein investigated organic thin film solar cells have five layers which are shown in Figure 1. The first layer is cathode, its function is to collect electrons. Then comes ETL, its basic function is to collect electrons from the absorber. The ETL is also known as the hole block layer. Absorber is the third layer (known as an active layer), when the light falls on the absorber charge carrier is produced, charge carrier are the combination of electron and hole. The fourth layer is HTL which is also used as electron blocking layer. It serves to extract the holes from the absorption layer. The final layer serves as an anode, with the function of collecting holes.

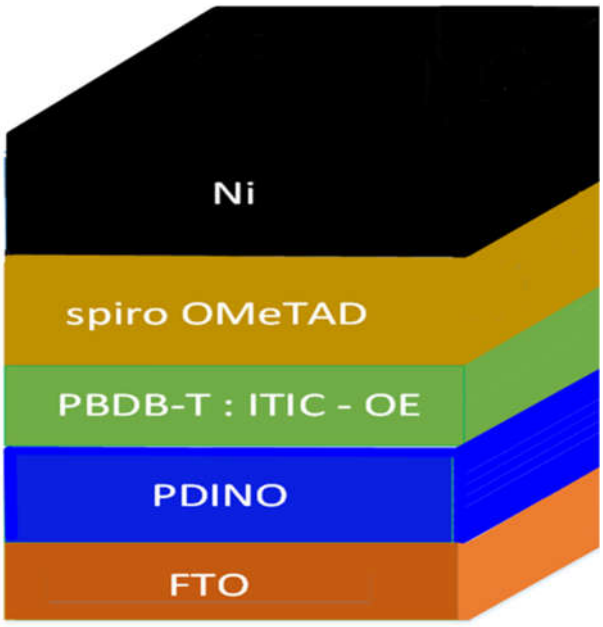

Figure 1. General structure for simulation with HTL, ETL and active layer.

Preprints (www.preprints.org) | NOT PEER-REVIEWED | Posted: 11 August 2023 doi:10.20944/preprints202308.0912.v1

Poly(2,2′-disulfonyl-4,4′-benzidineterephthalamide: (3,9-bis(2-methylene-(3-(1,1 dicyanomethy lene)-indanone)-5,5,11,11-tetraki (4-hexylphenyl)-dithieno[2,3-d:2,3-d]-s-indaceno[1,2-b:5,6-b]dithio phene oligoethylene)) (PBDT: ITIC-OE) is used as an active layer (active layer is the blend of donor and acceptor materials). PBDT is used as a donor material while ITIC: OE (oligoethylene side chain) is used as an acceptor. 2,2',7,7'-Tetrakis[N,N-di(4-methoxyphenyl)amino]-9,9'-spirobifluorene (spiro OMETAD) is applied as a HTL while N,N'-Bis(N,N-dimethylpropan-1-amine oxide)perylene-3,4,9,10-tetracarboxylic diimide (PDINO) is used as an ETL. Ni film is used as cathode while FTO is used as an anode. The energy states diagram of proposed organic solar cell is shown in Figure 2.

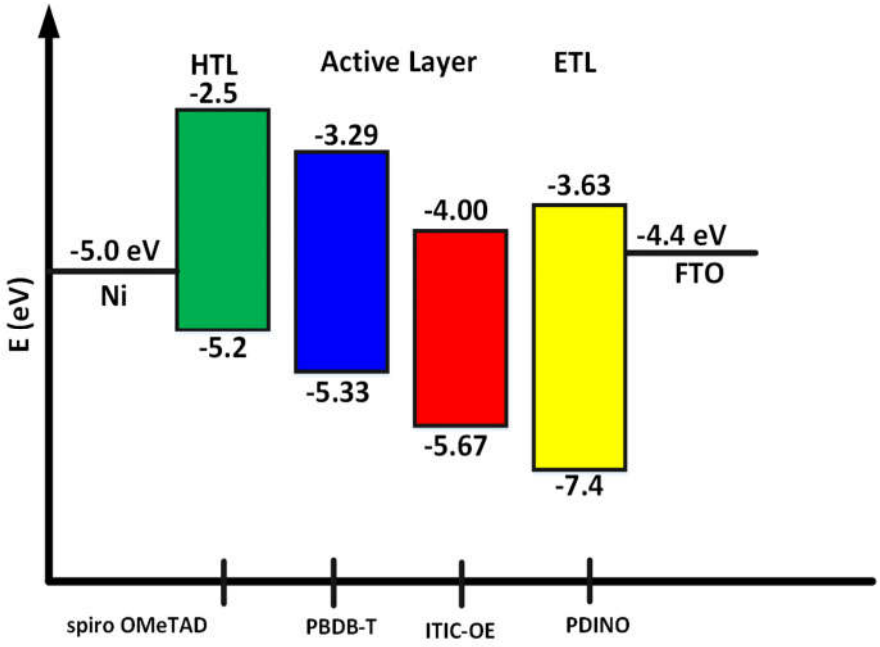

Figure 2. Energy states of OSC layers.

2.3. Parameters used in the simulation

All the values which are required for the simulation are collected from the literature. These values include band gap, electron and hole mobility, doping density, electron affinity, defect density for HTL, ETL and for the active layer blend. All the simulations are performed under the standard test conditions (STCS). The standard conditions are the air mass 1.5 G, temperature 300 K and irradiance 1000 w/m^2. The voltage value is set up to 1.3 V. The simulation parameters for active layer, HTL and ETL are presented in Table 1 while parameters for back contact and front contact electrode are presented in Table 2 and 3 respectively.

Table 1. Simulation Parameters for active layer, HTL and ETL.

Parameters	**Active layer** [19,29]	**HTL** [30]	**ETL** [31]
Thickness, d (nm)	80	50	50
Electron affinity, X (eV)	4.03	2.2	4.110
Energy band gap, Eg (eV)	1.2	2.9	2.98
Dielectric permittivity, ε	6.1	3	5
Valence band effective density of states, Nv (cm^{-3})	1E+19	1E+19	1E+19
Conduction band effective density of states, Nc (cm^{-3})	1E+19	1E+19	1E+19

Preprints (www.preprints.org) | NOT PEER-REVIEWED | Posted: 11 August 2023 doi:10.20944/preprints202308.0912.v1

Electron thermal velocity, Vth_e (cm/s),	1E+7	1E+7	1E+7
Hole thermal velocity, Vth_p (cm/s),	1E+7	1E+7	1E+7
Electron mobility, μ_n (cm^2/Vs)	1.2E-5	1E-4	2E-6
Hole mobility, μ_p (cm^2/Vs)	3.5E-4	2E-4	1E-3
Donor density, Nd ($1/cm^3$)	-	-	2E+21
Acceptor density, Na ($1/cm^3$)	-	2.8E+19	-
Defect density, Nt ($1/cm^3$)	1E+14	1E+14	1E+14

Table 2. Back Contact Properties of Electrode (Anode).

Parameters	**Values** [24]
Thermionic emission velocity for electron	1E+5 cm / sec
Thermionic emission velocity for hole	1E+7 cm / sec
Back electrode work function, Ni	5.01 eV

Table 3. Front Contact Properties of Electrode (Cathode).

Parameters	**Values** [24,27]
Thermionic emission velocity for electron	1E+7 cm / sec
Thermionic emission velocity for hole	1E+5 cm / sec
Front electrode work function, (FTO)	4.4 eV

3. Results and Discussions

3.1. J-V characteristics relation with energy band alignment

The J-V characteristics curve for the proposed structure was obtained and shown in Figure 3, while output performance parameters are shown in Table 4. Firstly, results are obtained for the optimized structure and then the reflection coating was applied to enhance the efficiency of this solar cell.

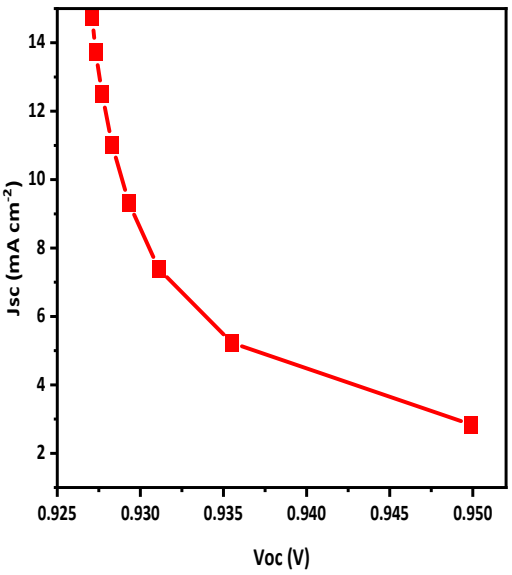

Figure 3. Characteristic J-V curve of simulated structure.

Preprints (www.preprints.org) | NOT PEER-REVIEWED | Posted: 11 August 2023 doi:10.20944/preprints202308.0912.v1

Table 4. Device performance parameters of optimized OSC before and after reflection coating.

Structure	Voc, (V)	Jsc (ma cm $^{-2}$)	FF (%)	η (%)
Before	0.927	14.763	49.98	6.84
After	0.939	21.654	46.2	9.40

Energy band alignment is critical to the performance of solar cells. Figure 4 contains the band alignment diagram for the HTL and ETL along with active layer. It shows that the HTL has maximum conduction band offset (CBO) and minimum valence band offset (VBO). On the other hand, the ETL has minimum CBO and maximum VBO.

Table 5 presents the CBO and VBO values of HTL and ETL. In Figure 4, Ec - represents conduction band offset, Fn - Fermi level of electrons, Fp - Fermi level of holes and Ev - valance band offset, respectively.

- **Ec**- In a semiconductor, the conduction band comprise of lowest occupied molecular orbital (LOMO). It is the highest energy level where the electrons can move freely within the solid [32].
- **Fn**- represents the n-type material Fermi level, where the probability of electron is 0.5. Fermi level is act as a boundary, it distinguishes the energy levels where electrons high likelihood of existence and from those where their presence is relatively unlikely. In an ETL or in n-type semiconductor, the Fn is close to conduction band due to surplus of electrons [32].
- **Fp**- represents the holes Fermi level, which is located near the valence band due to surplus of holes [32].
- **Ev**- In a solid ,the valence band represents the lowest energy level, where the electrons are tightly bound to the atoms and lack freedom of movement. In solar cells, this VB is comprised of the semiconductors materials highest occupied molecular orbital (HOMO) [32].

When the CB of the charge transport layer (CTL) and active layer are aligned, then there will be no hurdles to flow for the electron and the flow will be smooth. If the active layer CB is above the CB of ETL, it forms cliff interface which means negative conduction band offset (-CBO). The negative CBO reduces the performance of the solar cell. If the conduction band of the active layer is below the conduction band of HTL, then spike interface is formed. Spikes interfaces mean (+CBO) electron will flow smoothly but spikes can cause hurdles for the electrons to flow, and the recombination will occur.

Similarly, for the smooth flow of holes CTL valance band and active layer is aligned, if the active layer valence band (VB) is below the VB of the HTL, then cliff interface is formed (-VBO). The negative VBO reduces the performance of OSCs. If the active layer VB is above the VB of the ETL, then the spikes interface is formed. These spikes interface improves the performance of the solar cell. The CBO and VBO of the HTL and ETL along with active layer can be calculated by Anderson role. According to Anderson rule the offset can be calculated as [28]:

$$\mathrm{CBO} = (\mathrm{X\ active\ layer} - \mathrm{XCTL}) \quad (7)$$

In the above formula X represents electron affinity.

$$\mathrm{VBO} = (\mathrm{X\ CTL} - \mathrm{X\ active\ layer} + \mathrm{Eg\ CTL} - \mathrm{Eg\ active\ layer}) \quad (8)$$

In the above formula Eg represents the energy gap of CTL and active layer respectively.

Table 5. Obtained CBO and VBO of HTL and ETL values.

CTL	CBO	VBO
Spiro Ometad (HTL)	1.83	-0.13
PDINO (ETL)	-0.08	1.86

Preprints (www.preprints.org) | NOT PEER-REVIEWED | Posted: 11 August 2023 doi:10.20944/preprints202308.0912.v1

The ideal band gap alignment of the solar cell has maximum CBO, while minimum CBO of the ETL; while minimum VBO of the HTL and maximum VBO of the ETL.

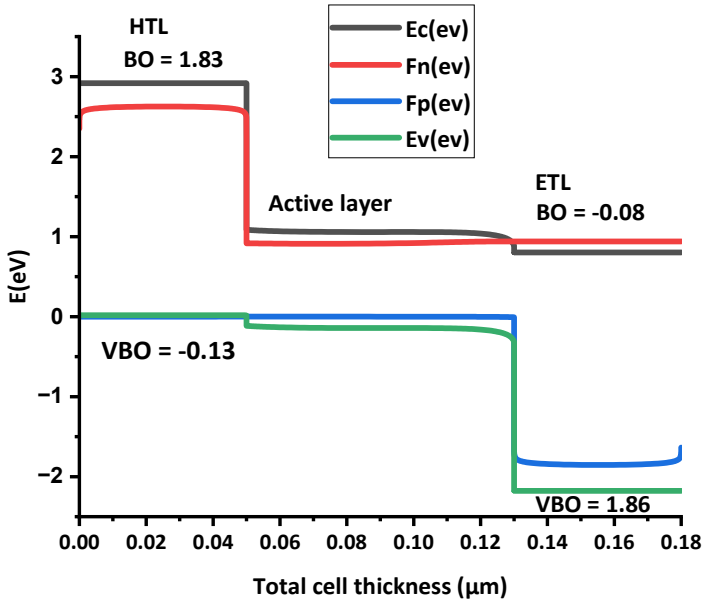

Figure 4. Energy band alignment of the HTL and ETL, along with the active layer.

3.2. Impact of active layer thickness on OSC

The thickness of HTL is optimized up to 50 nm at the start, however, it turned out that the HTL thickness has low influence on the device performance while ETL layer thickness is kept constant i.e., 50 nm. The thickness of the absorber is a critical factor in the photo absorption and generation process. When the film thickness is insufficient, it exhibits characteristics like a transparent film . Hence, we altered the thickness of the active layer in our simulation study ranging from 10 nm to 80 nm. The main purpose of this investigation was to assess its influence on solar cell performance and to enhance the electron-hole creation process. Figure 5, illustrates how the parameters change with varying active layer thickness. Specifically, it was observed that Voc and FF decrease while η and Jsc increases which, as depicted in Figure 5 (a-b) and (c-d) respectively. The decrease in Voc with increasing active layer thickness can be attributed to several factors. Firstly, thicker active layers charge carriers have to travel a longer distance from the photoactive layer to the respective electrodes, leading to increased resistance. Additionally, thicker layers may contain traps and defects that further reduce Voc. The decrease in FF is primarily due to an increase in series resistance, as the active layer thickness grows. This increase in resistance losses within the device can be attributed to factors such as the longer distance for charge carriers to travel, charge carrier trapping, and an increase in contact resistance at the electrodes. Despite the decrease in FF and Voc, the overall η and Jsc of the solar cell increases is due to increase in light absorption and generation of charge carriers.

Preprints (www.preprints.org) | NOT PEER-REVIEWED | Posted: 11 August 2023 doi:10.20944/preprints202308.0912.v1

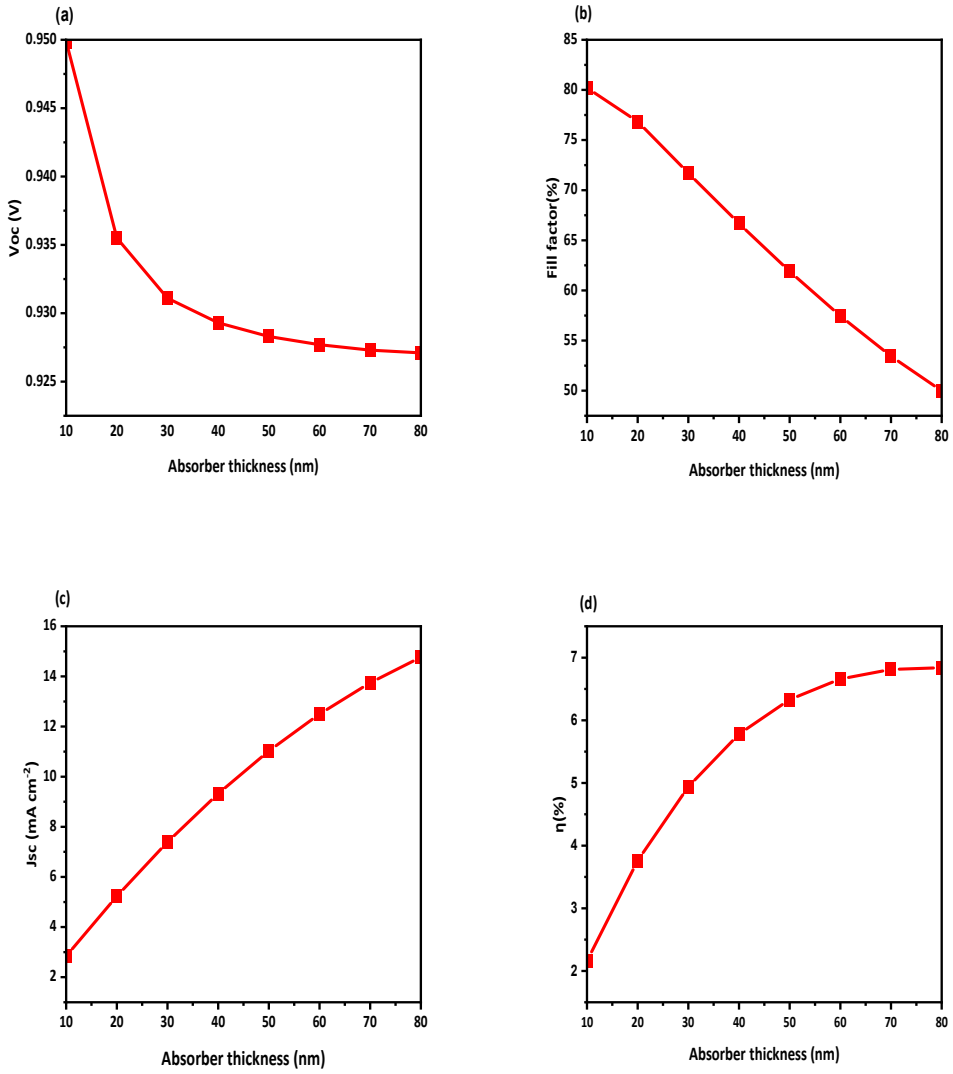

Figure 5. Effect of active layer thickness on photovoltaic parameters: a) Voc; b) FF; c) Jsc; d) η.

3.3. Active layer defect density effect on the performance of solar cell

The performance and outcomes of OSCs are significantly influenced by the structure and quality of the active layer. The defect density in the device is a crucial factor in achieving efficient results. Since polymers typically contain traps, our simulation incorporated a realistic Nt to accurately represent the system. The Nt depends on two parameters: 1) Quality of the active layer and 2) Preparation technique employed. A higher Nt value indicates an increased presence of light traps and crystal defects within the active layer. These traps hinder the movement of charges and promote recombination, ultimately affecting the solar cell's performance. Additionally, a higher Nt also influences the lifetime of charge carriers, causing a reduction in their longevity. Mathematically, this relationship is expressed as [28]:

$$\tau = \frac{1}{\sigma * Nt * Vth} \qquad (9)$$

In the equation (10), σ represents the capture cross-section, Nt stands for defect density and Vth denotes the thermal velocity associated with the carriers. The defect density (Nt) plays a crucial role in determining the recombination rate, known as Shockley-Red-hall recombination (R), which can be expressed as [33–35]:

Preprints (www.preprints.org) | NOT PEER-REVIEWED | Posted: 11 August 2023 doi:10.20944/preprints202308.0912.v1

$$R = \frac{np - ni^2}{\tau p\,(n+nt) + \tau n(P+Pt)} \quad (10)$$

where ni denotes intrinsic carrier concentration. n, np represents mobile carrier concentration and Pt refers to the trap defect concentration.

To investigate the impact of defect density (Nt) on the OSC structure, we varied Nt values from E14 to E18. Figure 6 (a-b) illustrates the influence of defect density on the Jsc and overall solar cell η. As the defect density (Nt) increases, there is a noticeable decrease in solar cell efficiency. After analyzing the results, we found that the optimized Nt value for this structure is E14.

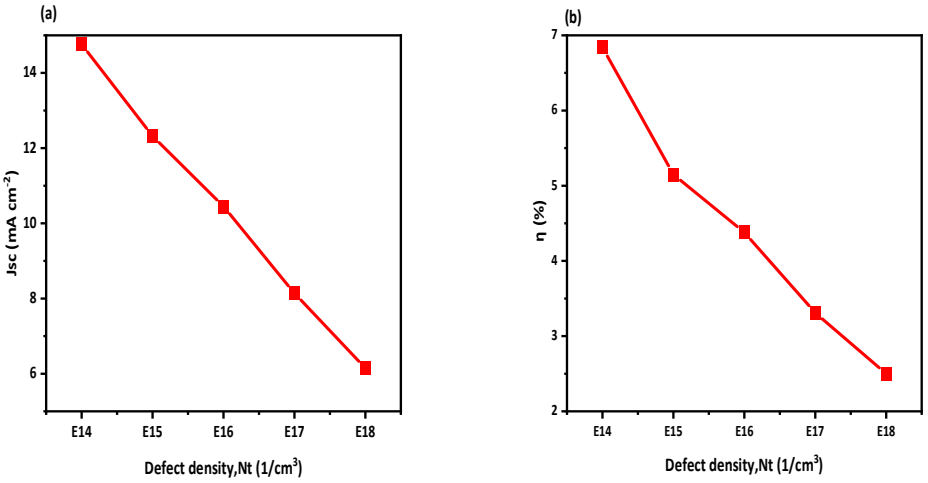

Figure 6. The graphs show how the active layer defect density influences photovoltaic parameters a) Jsc; b) PCE.

3.4. Effect of Temperature

Solar cells are mostly exposed to higher temperatures than ambient, thus understanding their impact on performance is essential. The ideal temperature for operating solar cells is room temperature, however the real temperature may vary between 300 to 400 K or maybe higher, so this simulation is performed by stepping up temperature from 300 K to 400 K. It is determined from the simulation results that temperature variations have an influence on the OSC performance. Figure 7(a-b) illustrates how temperature affects V_{oc} and η.

The decrease in Voc is due to the reverse saturation current density. Additionally, this phenomenon is further linked to the intrinsic carrier concentration (ni) and ni is related with band gap by the following mathematical relationship) [36].

$$ni^2 = K1e^{-Eg/KT} \quad (11)$$

where K1 is a constant.

Eg varies inversely proportional to the temperature as expressed by the mathematical equation [36].

$$E_g\,(T) = E_g\,(0) - \frac{\alpha T^2}{T+\beta} \quad (12)$$

α and β indicate the material constants While $E_g(0)$ refers to the band gap at temperature zero Kelvin.

Generally, the higher temperature means that more electrons will be excited due to which band gap may be unstable and the recombination of carrier increases and as a result the efficiency decreases.

Preprints (www.preprints.org) | NOT PEER-REVIEWED | Posted: 11 August 2023 doi:10.20944/preprints202308.0912.v1

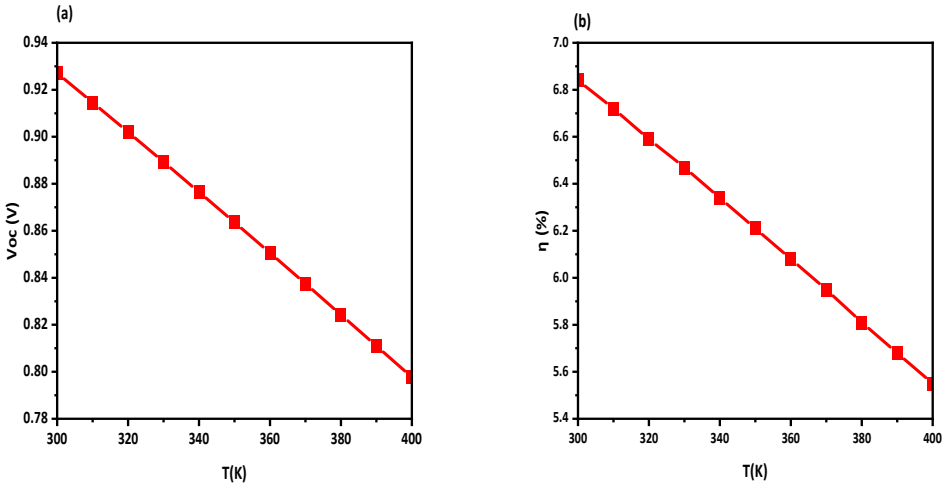

Figure 7. Effect of temperature on a) Voc; b) PCE.

3.5. Effect of Reflection Coating

Back-side reflection coating is a key method for increasing the effectiveness of absorption capacity and enhancing overall efficiency. In this technique backside reflective coating is deposited on it to enhance the optical length path. As we know that photons of larger wavelength (smaller energy) are absorbed by the absorber active layer, however, sometimes may not be quite absorbed. Adding the reflection coating, reflects those photons and moves towards absorber to increase the possibility of absorbance of those photons which improves the solar cell performance and efficiency [37]. In this simulation study Aluminum metal coating is considered due to its high reflectivity in the visible and near infrared region, however Gold (Au), and silver metal (Ag) can be also used. The reflective coating's back side is altered from 0 to 90% to study its effects. Figure 8 (a-b) shows that by adding reflection coating on backside of the solar cell improves the Jsc from 14.763 ma cm^{-2} to 21.654 ma cm^{-2} , as a result the efficiency of solar cell increases from 6.84 to 9.40.

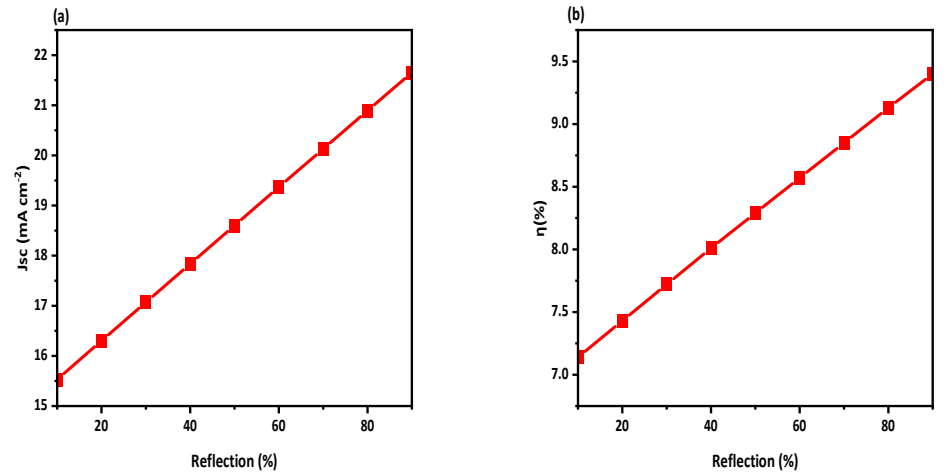

Figure 8. Effect of reflection coating on a) Jsc; b) PCE.

3.6. Hole transport layer doping density

The main purpose of the CTL in organic solar cells is to facilitation of ions movement smoothly from the absorption layer to respective electrodes. For efficient transport, the CTL layer has

Preprints (www.preprints.org) | NOT PEER-REVIEWED | Posted: 11 August 2023 doi:10.20944/preprints202308.0912.v1

maximum conductivity and minimum resistivity. This condition can be achieved through suitable doping. Due to doping concentration, the conductivity of CTL increases which increases the electric field at absorbing interface which increases the charge separation and increases the PCE of solar cell. Some materials show declination in performance at high doping due to mass Burstein effect [17]. The HTL doping value is taken from the literature which is 2.8E+19 cm^{-3} [31]. So, the value of NA is changed from E15 to E19 to examine this effect. Acceptor doping concentration affects the properties of solar cells, especially Voc and efficiency. By increasing NA, the efficiency and Voc of the structure is improved. The reason behind increasing the doping concentration is to boost the majority charge carriers, thereby enhancing the conductivity of the layer. This improved conductivity leads to a stronger electric field at the interface, promoting efficient ion separation. The impact of doping concentration on the Voc and PCE values is depicted in Figure 9 (a-b).

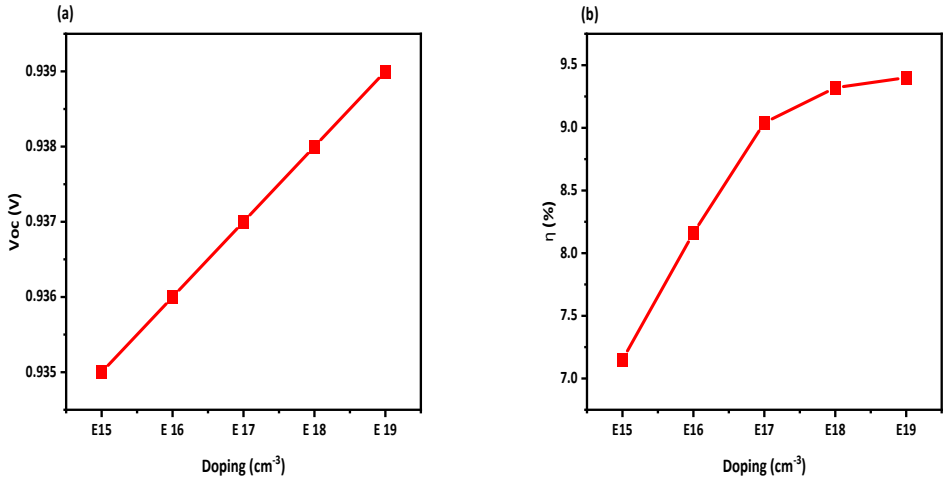

Figure 9. Doping density effect on a) Jsc; b) PCE.

3.7. Electron transport layer doping effect

The ETL doping value is changed from E17 to E21 to observe the effect of doping concentration on ETL parameters. When ND value is changed from E17 to E21, the Voc and efficiency increases which is evident from Figure **10 (a-b).** It is due to the majority charge carrier increases in the ETL and which improve the conductivity and electric field of the layer.

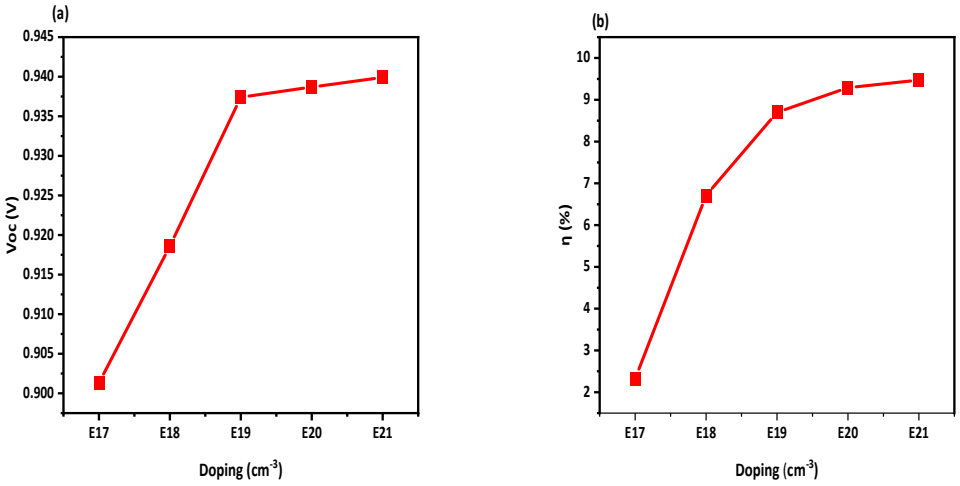

Figure 10. Doping density effect on a) Jsc; b) PCE.

Preprints (www.preprints.org) | NOT PEER-REVIEWED | Posted: 11 August 2023 doi:10.20944/preprints202308.0912.v1

3.8. Electric Field at interface

The efficiency of solar cells is significantly influenced by the electric field at the interface. When a high potential exists at the interface, charge carriers experience smooth separation and move toward their respective electrodes. Figure 11 illustrates the formation of two interfaces: HTL/active layer and ETL/active layer, each generating an electric field. The electric field at the ETL/active layer interface is stronger than the HTL/active layer interface, it may be due to high doping of ETL. This discrepancy means that the ETL contributes to enhanced charge separation within the active layer.

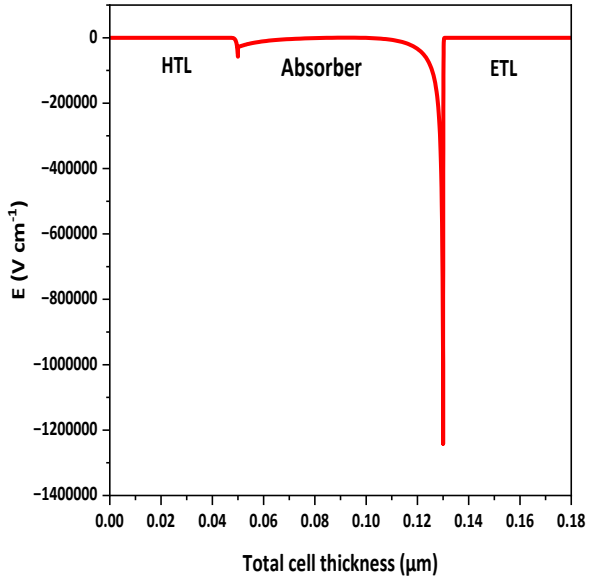

Figure 11. Distribution of electric potential at interfaces.

3.9. Comparison of simulation results with experimental studies

These simulation results are compared with the experimental studies reported in [5], for the same active layer used in photovoltaic device **(ITO/PEDOT: PSS/PBDB-T: ITIC-OE/PFN-Br/Ag)**. It is turned out that the obtained simulation results are in close agreement with the practical results. So, this software can be used for the performance enhancement of organic solar cells. The experimental and simulated results are shown in **Table 6.**

Table 6. Photovoltaic parameters determined for real structure and by simulation.

Parameters	**Experimental** [20]	**Simulated**
Voc	0.85	0.939
Jsc	14.8	21.654
FF	67.0	46.2
PCE	8.5	9.40

4. Conclusions

In this work, the BHJ polymer thin film solar cell: (ITO/PDINO/PBDB-T: ITIC-OE/ SPIRO OMETAD /Ni) was optimized and enhances its efficiency by changing the thickness of HTL and active layer, doping level and density of defects, through the presence of backside reflection coating. From these results it is shown that by increasing the thickness of active layer, Voc and FF decreases while Jsc and η increases. The reduction in Voc and FF is due to increase in the series resistance with thickness while Jsc and η increases due to the exciton formation. The active layer thickness was

optimized up to 80 nm. From the band gap alignment diagram, it is concluded that HTL has maximum CBO while minimum VBO while ETL have minimum CBO and maximum VBO, so there will be smoothly flow of electrons and holes.

Active layer defect density has noticeable impact on the solar cell performance, by increasing the defect density, the Jsc of the solar cell decreases which decreases the efficiency of the solar cell. The effect of temperature on solar cells is also studied by increasing the temperature and the performance of solar cell reduces such as efficiency and Jsc decreases with increase of temperature. Back side reflection coating is applied on the back side of solar cell which improves the efficiency and Jsc of the solar cell. The efficiency increases by 2.5 % by applying the back side reflection layer while overall efficiency is achieved as 9.4 %. Moreover, it is turns out that the HTL and ETL doping improve the Voc and efficiency of the solar cell. During simulation the HTL doping density was varied from E15 to E19, while ETL doping density was from E17 to E21. It is observed that HTL doping increased Voc from 0.935 to 0.939 and efficiency from 7.15 to 9.4. Similarly, ETL doping raised Voc from 0.921 to 0.939 and efficiency from 2.3 to 9.4.

Additionally, these obtained simulation results are compared with the practical results which are available in the literature. From these simulation studies it is concluded that this software can be successfully used for the optimization and performance enhancement of organic solar cells. Results of our simulations confirm the role of the presence of reflection coating, thickness of active layer, temperature, and doping level on photovoltaic parameters of (PBDT: ITIC-OE) based BHJ organic solar cells.

Author Contributions: M.R.K-conceptualization, methodology,writing original draft; B.J-conceptualization, supervision, writing-review and editing.

Funding: This research received no external funding.

Institutional Review Board Statement: Not applicable.

Conflicts of Interest: The authors declares no conflict of interest.

References

1. Alahmadi, A. N. (2022). Design of an efficient PTB7: PC70BM-based polymer solar cell for 8% efficiency. *Polymers*, *14*(5), 889.
2. Seri, M., Mercuri, F., Ruani, G., Feng, Y., Li, M., Xu, Z. X., & Muccini, M. (2021). Toward real setting applications of organic and perovskite solar cells: A comparative review. *Energy Technology*, *9*(5), 2000901.
3. Peng, W., Lin, Y., Jeong, S. Y., Genene, Z., Magomedov, A., Woo, H. Y., ... & Wang, E. (2022). Over 18% ternary polymer solar cells enabled by a terpolymer as the third component. *Nano Energy*, *92*, 106681.
4. Ghosekar, I. C., & Patil, G. C. (2021). Review on performance analysis of P3HT: PCBM-based bulk heterojunction organic solar cells. *Semiconductor Science and Technology*, *36*(4), 045005.
5. Moiz, S. A., Alahmadi, A. N. M., & Karimov, K. S. (2020). Improved organic solar cell by incorporating silver nanoparticles embedded polyaniline as buffer layer. *Solid-State Electronics*, *163*, 107658.
6. Li, W., Ye, L., Li, S., Yao, H., Ade, H., & Hou, J. (2018). A high-efficiency organic solar cell enabled by the strong intramolecular electron push–pull effect of the nonfullerene acceptor. *Advanced Materials*, *30*(16), 1707170.
7. Fan, X., Zhang, M., Wang, X., Yang, F., & Meng, X. (2013). Recent progress in organic–inorganic hybrid solar cells. *Journal of Materials Chemistry A*, *1*(31), 8694-8709.
8. Chen, C. C., Chang, W. H., Yoshimura, K., Ohya, K., You, J., Gao, J., … & Yang, Y. (2014). An efficient triple-junction polymer solar cell having a power conversion efficiency exceeding 11%. *Advanced materials*, *26*(32), 5670-5677.
9. Malik, A., Hameed, S., Siddiqui, M. J., Haque, M. M., Umar, K., Khan, A., & Muneer, M. (2014). Electrical and optical properties of nickel-and molybdenum-doped titanium dioxide nanoparticle: improved performance in dye-sensitized solar cells. *Journal of materials engineering and performance*, *23*, 3184-3192.
10. R. Murad, A., Iraqi, A., Aziz, S. B., N. Abdullah, S., & Brza, M. A. (2020). Conducting polymers for optoelectronic devices and organic solar cells: A review. *Polymers*, *12*(11), 2627.
11. Sharma, N., Gupta, S. K., & Negi, C. M. S. (2019). Influence of active layer thickness on photovoltaic performance of PTB7: PC70BM bulk heterojunction solar cell. *Superlattices and Microstructures*, *135*, 106278.

12. Ramírez-Como, M., Balderrama, V. S., Sacramento, A., Marsal, L. F., Lastra, G., & Estrada, M. (2019). Fabrication and characterization of inverted organic PTB7: PC70BM solar cells using Hf-In-ZnO as electron transport layer. *Solar Energy*, *181*, 386-395.
13. Dridi, C., Touafek, N., & Mahamdi, R. (2022). Inverted PTB7: PC70BM bulk heterojunction solar cell device simulations for various inorganic hole transport materials. *Optik*, *252*, 168447.
14. Chen, J., Chen, Y., Feng, L. W., Gu, C., Li, G., Su, N., ... & Marks, T. J. (2020). Hole (donor) and electron (acceptor) transporting organic semiconductors for bulk-heterojunction solar cells. *EnergyChem*, *2*(5), 100042.
15. Su, G. M., Pho, T. V., Eisenmenger, N. D., Wang, C., Wudl, F., Kramer, E. J., & Chabinyc, M. L. (2014). Linking morphology and performance of organic solar cells based on decacyclene triimide acceptors. *Journal of Materials Chemistry A*, *2*(6), 1781-1789.
16. Cui, Y., Yao, H., Zhang, J., Xian, K., Zhang, T., Hong, L., … & Hou, J. (2020). Single-junction organic photovoltaic cells with approaching 18% efficiency. *Advanced Materials*, *32*(19), 1908205.
17. Yan, C., Barlow, S., Wang, Z., Yan, H., Jen, A. K. Y., Marder, S. R., & Zhan, X. (2018). Non-fullerene acceptors for organic solar cells. *Nature Reviews Materials*, *3*(3), 1-19.
18. Ma, L., Zhang, S., Wang, J., Xu, Y., & Hou, J. (2020). Recent advances in non-fullerene organic solar cells: From lab to fab. *Chemical Communications*, *56*(92), 14337-14352.
19. Liu, X., Xie, B., Duan, C., Wang, Z., Fan, B., Zhang, K., ... & Cao, Y. (2018). A high dielectric constant non-fullerene acceptor for efficient bulk-heterojunction organic solar cells. *Journal of Materials Chemistry A*, *6*(2), 395-403.
20. Torabi, S., Jahani, F., Van Severen, I., Kanimozhi, C., Patil, S., Havenith, R. W., ... & Koster, L. J. A. (2015). Strategy for enhancing the dielectric constant of organic semiconductors without sacrificing charge carrier mobility and solubility. *Advanced Functional Materials*, *25*(1), 150-157.
21. Alam, S., Akhtar, M. S., Shin, H. S., & Ameen, S. (2020). New energetic indandione based planar donor for stable and efficient organic solar cells. *Solar Energy*, *201*, 649-657.
22. Akhtar, M. S., Kim, E. B., Fijahi, L., Shin, H. S., & Ameen, S. (2020). A symmetric benzoselenadiazole based D–A–D small molecule for solution processed bulk-heterojunction organic solar cells. *Journal of Industrial and Engineering Chemistry*, *81*, 309-316.
23. Abdelaziz, W., Zekry, A., Shaker, A., & Abouelatta, M. (2020). Numerical study of organic graded bulk heterojunction solar cell using SCAPS simulation. *Solar Energy*, *211*, 375-382.
24. Nowsherwan, G. A., Samad, A., Iqbal, M. A., Mushtaq, T., Hussain, A., Malik, M., ... & Choi, J. R. (2022). Performance analysis and optimization of a PBDB-T: ITIC based organic solar cell using graphene oxide as the hole transport layer. *Nanomaterials*, *12*(10), 1767.
25. Bendenia, C., Merad-Dib, H., Bendenia, S., Bessaha, G., & Hadri, B. (2021). Theoretical study of the impact of the D/A system polymer and anodic interfacial layer on inverted organic solar cells (BHJ) performance. *Optical Materials*, *121*, 111588.
26. Nithya, K. S., & Sudheer, K. S. (2020). Device modelling of non-fullerene organic solar cell with inorganic CuI hole transport layer using SCAPS 1-D. *Optik*, *217*, 164790.
27. Jan, S. T., & Noman, M. (2022). Influence of absorption, energy band alignment, electric field, recombination, layer thickness, doping concentration, temperature, reflection and defect densities on MAGeI3 perovskite solar cells with Kesterite HTLs. *Physica Scripta*, *97*(12), 125007.
28. Ahmad, W., Noman, M., Tariq Jan, S., & Khan, A. D. (2023). Performance analysis and optimization of inverted inorganic CsGeI3 perovskite cells with carbon/copper charge transport materials using SCAPS-1D. *Royal Society Open Science*, *10*(3), 221127.
29. Nithya, K. S., & Sudheer, K. S. (2022). Device modelling and optimization studies on novel ITIC-OE based non-fullerene organic solar cell with diverse hole and electron transport layers. *Optical Materials*, *123*, 111912.
30. Salem, M. S., Shaker, A., & Salah, M. M. (2023). Device Modeling of Efficient PBDB-T: PZT-Based All-Polymer Solar Cell: Role of Band Alignment. *Polymers*, *15*(4), 869.
31. Abdelaziz, W., Zekry, A., Shaker, A., & Abouelatta, M. (2020). Numerical study of organic graded bulk heterojunction solar cell using SCAPS simulation. *Solar Energy*, *211*, 375-382.
32. Ismail, M., Noman, M., Tariq Jan, S., & Imran, M. (2023). Boosting efficiency of eco-friendly perovskite solar cell through optimization of novel charge transport layers. *Royal Society Open Science*, *10*(6), 230331.
33. Gan, Y., Qiu, G., Qin, B., Bi, X., Liu, Y., Nie, G., ... & Yang, R. (2023). Numerical Analysis of Stable (FAPbI3) 0.85 (MAPbBr3) 0.15-Based Perovskite Solar Cell with TiO2/ZnO Double Electron Layer. *Nanomaterials*, *13*(8), 1313.
34. Sherkar, T. S., Momblona, C., Gil-Escrig, L., Avila, J., Sessolo, M., Bolink, H. J., & Koster, L. J. A. (2017). Recombination in perovskite solar cells: significance of grain boundaries, interface traps, and defect ions. *ACS energy letters*, *2*(5), 1214-1222.
35. Haider, S. Z., Anwar, H., & Wang, M. (2018). A comprehensive device modelling of perovskite solar cell with inorganic copper iodide as hole transport material. *Semiconductor Science and Technology*, *33*(3), 035001.

 doi:10.20944/preprints202308.0912.v1

36. Khan, A. D., Subhan, F. E., Khan, A. D., Khan, S. D., Ahmad, M. S., Rehan, M. S., & Noman, M. (2020). Optimization of efficient monolithic perovskite/silicon tandem solar cell. *Optik*, *208*, 164573.
37. Jan, S. T., & Noman, M. (2022). Influence of layer thickness, defect density, doping concentration, interface defects, work function, working temperature and reflecting coating on lead-free perovskite solar cell. *Solar Energy*, *237*, 29-43.